# Study of Anomalous S-shape in Current Density-Voltage Characteristics of Carrier Selective Contact Molybdenum Oxide and Amorphous Silicon based Heterojunction Silicon Solar Cells

Sapna Mudgal<sup>a)</sup>, Mrutyunjay Nayak, Sonpal Singh and Vamsi K. Komarala

Centre for Energy Studies, Indian Institute of Technology Delhi, India.

a)sapnamudgal89@gmail.com

**Abstract.** We have investigated charge carrier recombination and transport mechanism in heterojunction silicon solar cells of different configurations like; Ag/ITO/a-Si:H(p+)/a-Si:H(i)/c-Si(n)/a-Si:H(n+)/ITO/Ag (SHJ cell) and Ag/ITO/MoOx/c-Si(n)/LiFx/Al (MoOx cell). Two cells having S-shape in light current density—voltage (J-V) characteristics are analyzed by the Suns-Voc, and quantum efficiency with voltage- and light-bias measurements. The MoOx cell has shown turn-around in the Suns-Voc graph, whereas a linear behaviour has been observed from the SHJ cell. Quantum efficiency analysis has revealed poor performance of the MoOx cell from the back-side, for this cell the minority carrier diffusion lengths also is estimated. The S-shape in light J-V graph of MoOx cell is due to carrier extraction barrier for trap assisted tunneling at the MoOx/c-Si interface by the insufficient number of traps, which also is reflected as turn-around in the Suns-Voc characteristics. Whereas; the S-shape in J-V graph of SHJ cell is due to minority charge carrier barrier from the band-offset at a-Si/c-Si junction instead of the Schottky contact barrier, since no turn-around in the Suns-Voc graph.

### INTRODUCTION

Carrier-selective contact based silicon heterojunction (SHJ) solar cells have got an attention due to the better performance over the conventional silicon solar cells. However, the carrier collection/transport is an issue in such cells, and show a non-ideal behavior in light current density-voltage (J-V) graphs due to energy band-offset and carrier-selective materials' work function variation (depends on preparation method, material stoichiometry and structure) with a crystalline silicon. The material electronic properties variation can lead to the S-shape in light J-V graph rather than conventional J-shape, and hence severely affect a fill factor and overall performance of a SHJ cell. The S-shape in the J-V graphs are observed in case of amorphous silicon/crystalline silicon (a-Si:H/c-Si) [1, 2], and MoOx/c-Si SHJ solar cells [3, 4].

In this work; we have investigated carrier recombination and transport mechanism of Ag/ITO/a-Si:H(p+)/a-Si:H(i)/c-Si(n)/a-Si:H(n+)/ITO/Ag (SHJ) and Ag/ITO/MoO<sub>x</sub>/c-Si(n)/LiF<sub>x</sub>/Al (MoO<sub>x</sub>) solar cells having a moderate conversion efficiency. The anomalous S-shape characteristics in J-V graphs are analyzed by the Suns-V<sub>OC</sub> and quantum efficiency measurements.

# **EXPERIMENTAL DETAILS**

For this study; cells consisting of Ag/ITO/a-Si:H(p+)/a-Si:H(i)/c-Si(n)/a-Si:H(n+)/ITO/Ag (SHJ cell), and Ag/ITO/MoO<sub>x</sub>/c-Si(n)/LiF<sub>x</sub>/Al (MoO<sub>x</sub> cell) were fabricated on chemically cleaned and textured Cz n-type Si wafers. All amorphous silicon layers were deposited by plasma enhanced chemical vapor deposition (PECVD) system, the Indium Tin Oxide (ITO) was deposited using RF magnetron sputtering system. The MoO<sub>x</sub> and LiF<sub>x</sub> films, front and back metal contacts were deposited by thermal evaporation system. The thickness of MoO<sub>x</sub> and LiF<sub>x</sub> layers are ~20

nm and  $\sim$ 1 nm, and a-Si:H (i) and a-Si:H (p+) layers are  $\sim$ 11 nm and  $\sim$ 10 nm, respectively. The cell's J-V graphs were recorded under dark and light (1000 W/m²) by the Oriel (Class AAA) solar simulator along with the Keithley 2440 as a source meter. The Suns-V<sub>OC</sub> graphs were recorded by the Sinton WCT-120 TS, and external quantum efficiency (EQE) spectra were recorded at different DC voltage and light bias conditions by the ReRa (SpeQuest) system.

## RESULTS AND DISCUSSION

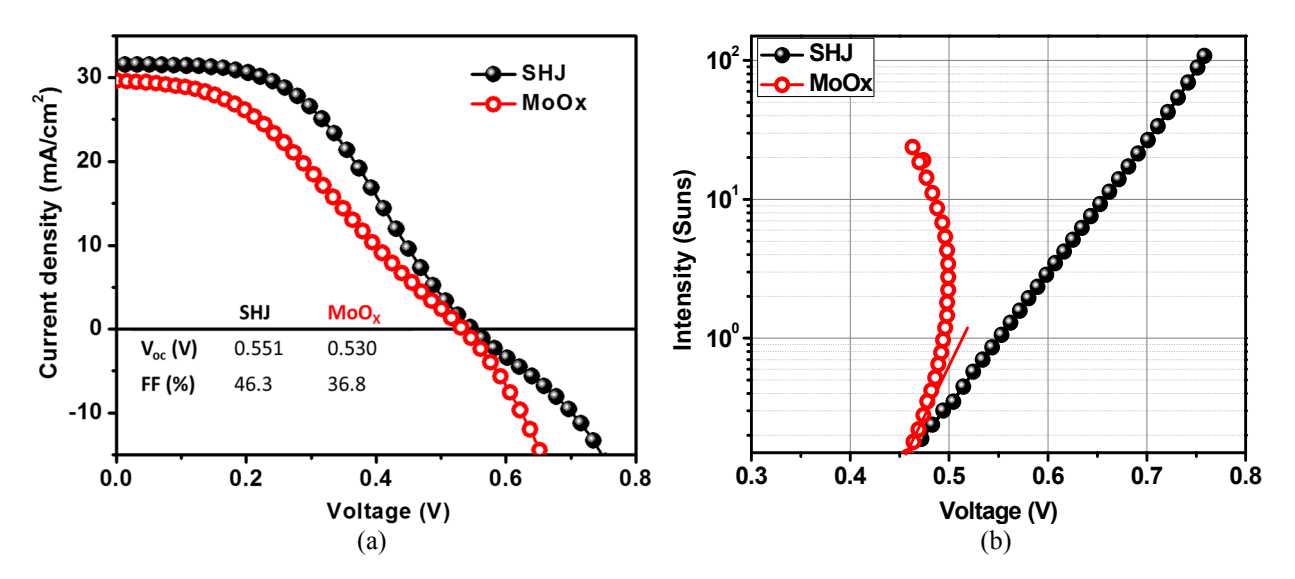


FIGURE 1. (a) Current density-voltage graphs under light, and (b) incident light intensity versus open-circuit voltage (Suns-V<sub>OC</sub>) graphs of SHJ and MoO<sub>x</sub> cells.

Figure 1 shows the J-V graphs under light, and incident light intensity versus open-circuit voltage (Suns- $V_{OC}$ ) graphs of SHJ and  $MoO_x$  cells. Both cells have shown the S-shape in light J-V graphs (Fig. 1a), and inset of the table shows cells' fill factor and  $V_{oc}$  parameters. The anomalous S-shape in light J-V graphs is due to the presence of carrier injection and/or extraction barriers, which create an imbalance of photogenerated minority charge carriers for transport [1-4]. In the Suns- $V_{OC}$  graphs (with an increase of light intensity up to 100 suns), the SHJ cell has shown a linear increase in the  $V_{oc}$ , whereas the  $MoO_x$  cell has shown a non-linear  $V_{oc}$  behaviour (even before 1 sun a decrease in  $V_{oc}$ ). The turn-around behaviour of  $V_{oc}$  in case of  $MoO_x$  cell can be due to the presence of one type of barrier at  $MoO_x/Si$  junction for carrier transport, which opposes the flow of minority charge carriers leading to a drop in the  $V_{oc}$  with an increase of light intensity [5], which is not present in the SHJ cell. We try to resolve type of minority charge carrier barrier at the junction by voltage and light bias dependent quantum efficiency analysis.

# **Quantum Efficiency Analysis Under Short Circuit Condition**

Figure 2a shows the internal quantum efficiency (IQE) spectra of both cells, a remarkable difference in the spectra is observed in the broad polychromatic spectral region. The MoO<sub>x</sub> cell's IQE is better than the SHJ cell in the shorter wavelength region due to the parasitic absorption loss minimization. Whereas; at the longer wavelength region, the SHJ cell's IQE response is better than the MoO<sub>x</sub> cell due to the minimal charge carrier recombination loss at the rearside. The cells are investigated further by the inverse IQE versus absorption depth plots for the minority carrier diffusion lengths estimation (Fig. 2b). The effective diffusion lengths ( $L_{\rm eff}$ ) are estimated using the relation cited in the reference [6], which are ~100  $\mu$ m and ~810  $\mu$ m for the MoO<sub>x</sub> and SHJ cells, respectively. The smaller  $L_{\rm eff}$  of the MoO<sub>x</sub> cell is an indication of an inefficient surface passivation by the LiF<sub>x</sub> layer leading large surface recombination at the rear-side. On the other hand, the SHJ cell has shown relatively better rear-side passivation than the MoO<sub>x</sub> cell even without the buffer intrinsic amorphous silicon layer.

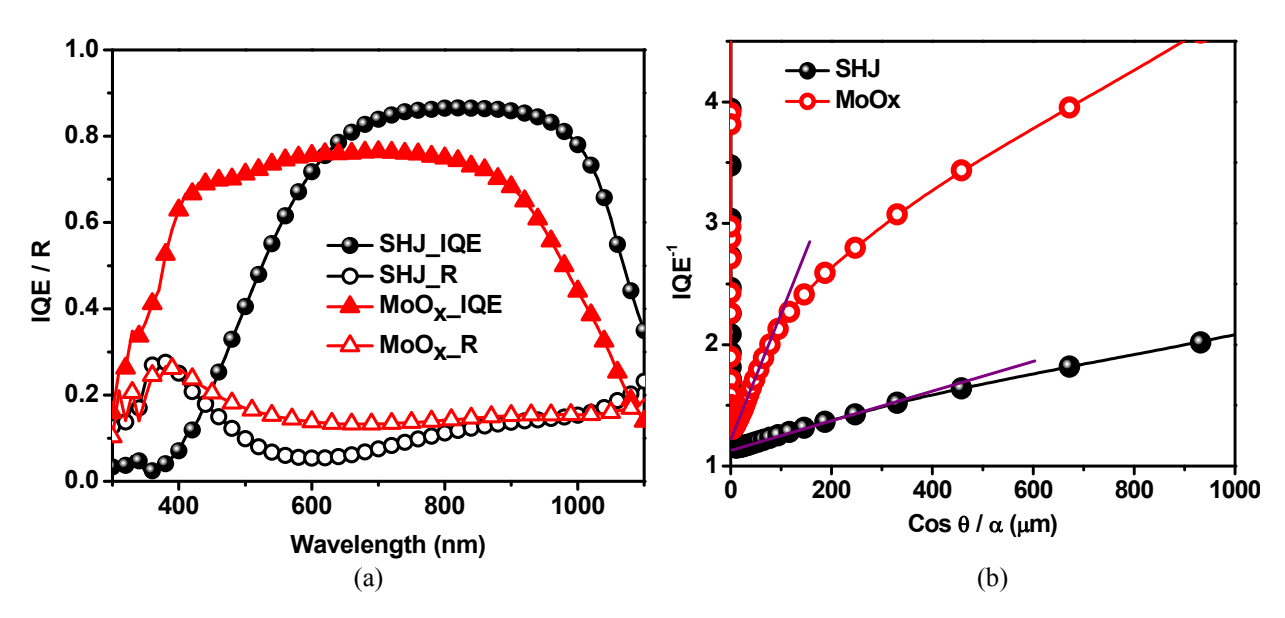
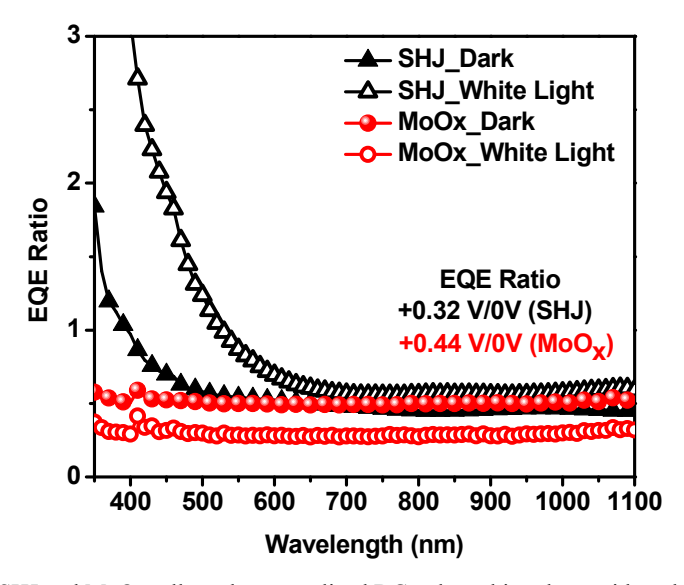


FIGURE 2. (a) IQE and total reflectance spectra, and (b) estimated effective minority carrier diffusion lengths of SHJ and MoO<sub>x</sub> cells

# DC Voltage and Light Bias Dependent Quantum Efficiency Analysis



**FIGURE 3.** EQE spectra of SHJ and MoO<sub>x</sub> cells under normalized DC voltage bias along with and without white light bias, first the EQE spectra of SHJ and MoO<sub>x</sub> cells are obtained with 0.32 V and 0.44 V bias conditions, respectively, and then the spectrum is normalized to the without voltage bias EQE spectrum of each cell.

Initially, the EQE spectra for both cells are recorded without voltage bias. Then the DC bias voltage is applied by considering the voltage where the S-shape has started appearing in the light J-V graphs ( $\sim$ 0.32 V for SHJ cell and  $\sim$ 0.44 V for MoO<sub>x</sub> cell). The EQE spectrum of cell with the voltage bias will provide the better understanding of charge carrier recombination/collection process at a main junction [1, 2]. The DC voltage biased EQE spectrum is normalized to the without voltage EQE spectrum, and spectra are presented in the Fig. 3. The normalized EQE spectrum has reduced to a half instead of unity (except below 500 nm wavelength region for the SHJ cell) with the bias voltage, which is an indication of non-ideal behaviour of both the junctions. In case of the SHJ cell, the normalized EQE value in the shorter wavelength region >0.5 is an indication of the defective nature of a-Si layers [2].

Along with the chosen voltage bias, the DC white light bias also is applied while recording the EQE spectrum, the spectra are presented in the Fig. 3. The EQE spectra of both cells have shown an opposite trend with the white light bias in the entire wavelength region.

In case of the SHJ cell, the EQE under white light bias is higher than without light bias condition due to the saturation of some of the defect states in the a-Si layers [2]. On the other hand, the  $MoO_x$  cell has shown the uniform reduction in entire EQE spectrum under white light bias. The  $MoO_x$  layer is transparent to the incident light, so, the light absorption happens only in the silicon base material. The barrier for charge carrier collection is outside the light absorption region this affects the collection of charge carriers. If the  $MoO_x$  film's work function is less than the optimum with respect to the c-Si, which can restrict carrier collection due to insufficient number of traps states for trap assisted tunnelling [3]. Since the  $LiF_x$  film contact resistance is small this cannot produce contact barrier [7], insufficient number of traps for trap assisted tunnelling appears to be the most probable reason for the S-shape in  $MoO_x$  cell. The structures used for analysis and nature of charge carrier's accumulation are shown in Fig. 4 through the energy band diagrams. Since, the contact barrier is not observed for the minority charge carriers in SHJ cell, therefore, the large band offset at the a-Si/c-Si junction along with defected a-Si:H is the most probable reason for the S-shape behaviour [1, 2].

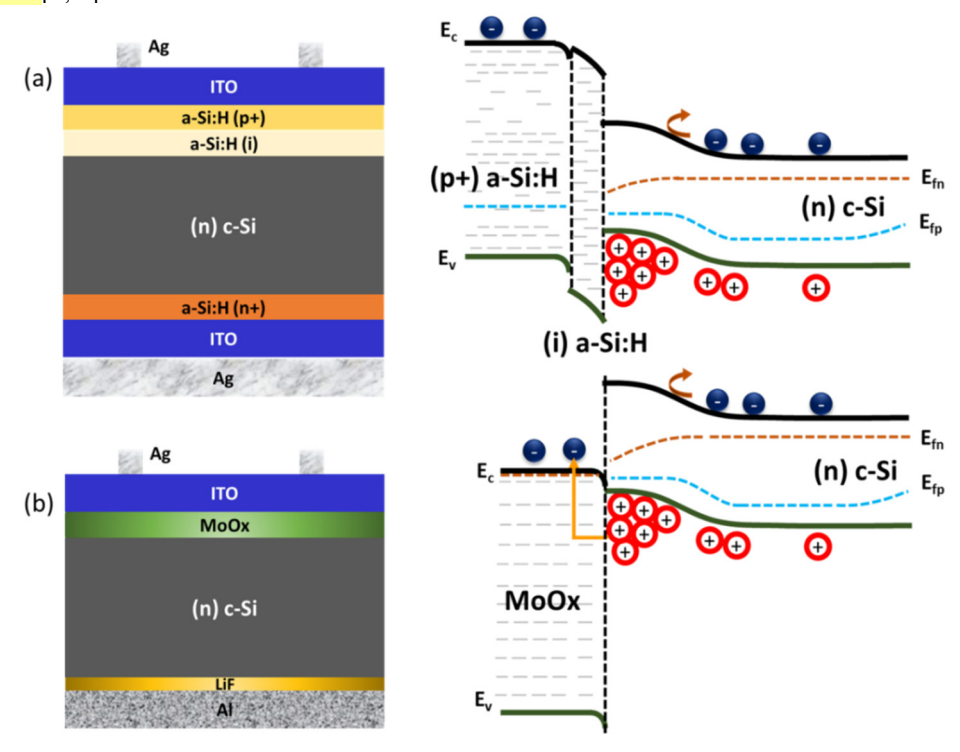


**FIGURE 4.** Cells' schematics and energy band diagram of front junction under illumination and forward voltage bias conditions; (a) SHJ cell and (b) MoOx cell.

## **CONCLUSIONS**

We have analyzed the SHJ and  $MoO_x$  cells having S-shapes in their light current density-voltage graphs using Suns-V<sub>oc</sub> and quantum efficiency under voltage and light bias conditions. The EQE spectra have shown different behavior for the SHJ and  $MoO_x$  cells under voltage and light bias. In case of SHJ cell, the charge carrier collection issue is correlated to band offset at the front junction, whereas for the  $MoO_x$  cell it is due to the restricted charge collection by the lack of enough trap states in the  $MoO_x$  for carrier tunneling.

#### ACKNOWLEDGMENTS

Authors would like to thank Department of Science and Technology of India for their financial support under Clean Energy Research Initiative grant (CERI grant number RP03240). Sapna Mudgal would like to thank University Grant Commission (UGC), India for a financial assistantship for this research work. The authors acknowledge amorphous silicon R & D plant of Bharat Heavy Electrical Limited (BHEL), India for providing the SHJ cells.

#### REFERENCES

- 1. U. K. Das, S. S. Hegedus, L. Zhang, J. Appel, J. Rand, and R. W. Birkmire, in *35th IEEE Photovoltaic Specialists Conference Proceedings*, IEEE Journal of Selected Topics in Quantum Electronics 2010, 001358-001362.
- 2. S. Mudgal, S. Sonpal, and V. K. Komarala, IEEE J. Photovolt. 8(4), 909-915 (2018).
- 3. R. A. Vijayan, S. Essig, S De Wolf, B.G. Ramanathan, P. Löper, C. Ballif and M. V. Perumal, IEEE J. Photovolt. **8(2)**, 473-482 (2018).
- 4. C. Battaglia, S. M. De Nicolas, S. De Wolf, X. Yin, M. Zheng, C. Ballif, and A. Javey, Appl. Phys. Letters 104(11), 113902 (2014).
- 5. O. Gunawan, T. Gokmen, and D.B. Mitzi, J. Appl. Phys. **116(8)**, 084504 (2014).
- 6. R. Brendel, "Advanced Quantum Efficiency Analysis," in *Thin-film Crystalline Silicon Solar Cells: Physics and Technology* (John Wiley and Sons, USA, 2005), pp. 53–89.
- 7. M. Nayak, K. Singh, S. Mudgal, S. Mandal, S. Singh, and V. K. Komarala, Phys. Status Solidi (a). 1900208 (2019), DOI: 10.1002/pssa.201900208.